Photoacoustic imaging of breast microcalcifications: A preliminary study with 8-gauge core-biopsied breast specimens

Ga Ram Kim

Department of Medicine

The Graduate School, Yonsei University

Photoacoustic imaging of breast microcalcifications: A preliminary study with 8-gauge core-biopsied breast specimens

Ga Ram Kim

Department of Medicine

The Graduate School, Yonsei University

Photoacoustic imaging of breast microcalcifications: A preliminary study with 8-gauge core-biopsied breast specimens

Directed by Professor Eun-Kyung Kim

The Doctoral Dissertation
submitted to the Department of Medicine,
the Graduate School of Yonsei University
in partial fulfillment of the requirements for the degree
of Doctor of Philosophy

Ga Ram Kim

December 2013

This certifies that the Master's Thesis (Doctoral Dissertation) of Ga Ram Kim is approved.

Thesis Supervisor : Eun-Kyung Kim

Thesis Committee Member#1 : Jin Young Kwak

Thesis Committee Member#2 : Jin Ho Chang

Thesis Committee Member#3: Seung Il Kim

Thesis Committee Member#4: Ji Hyun Youk

The Graduate School
Yonsei University

December 2013

ACKNOWLEDGEMENTS

I acknowledge my deep gratitude to Professer Eun-Kyung Kim, who is my thesis director, for supporting my efforts with total commitment and facilitating every step of the process. My appreciation for her guidance and encouragement is tremendous. I am also indebted to Professor Jin Young Kwak and Professor Jin Ho Chang for their great help for pertinent advice to assure the superior quality of this paper. Additionally, I thank Professor Seung Il Kim, Professor Ji Hyun Youk and Professor Hee Jung Moon for their sincere advice.

<TABLE OF CONTENTS>

ABSTRACT 1
I. INTRODUCTION 3
II. MATERIALS AND METHODS
1. StudySample 4
2. Imaging System and Experimental Procedures 5
3. Data Analyses 8
III. RESULTS
1. Baseline Characteristics 9
2. Detection of Microcalcifications on Photoacoustic Images 10
3. Comparison of Quantitative Photoacoustic Spectral Responses 15
IV. DISCUSSION 17
V. CONCLUSION 20
REFERENCES 21
ABSTRACT (IN KOREAN) 24

LIST OF FIGURES

Figure 1. Diagram demonstrates experimental arrangement 6
Figure 2. Representative case from ex vivo experiments with core specimens of breast tissue included in the microcalcification group (case #2) 12
Figure 3. Representative case from ex vivo experiments with core specimens of breast tissue included in the control group (case #5) 13
Figure 4. Spectral change in mean values of the maximum photoacoustic signals at the 700 nm and 800 nm wavelength sections in the control and microcalcification group 14
Figure 5. The PAI ratio in the microcalcification group was significantly higher than that in the control group 16

LIST OF TABLES

Table 1. Baseline characteristics of 21 cases of the control and microcalcification groups 9
Table 2. Results of blind review to assume calcification on PAI 11
Table 3. PAI ratios from regions of interest within each core 15
Table 4. Multiple regression analysis in the microcalcification group (n=11) to find factors that contribute to PAI ratios 16

ABSTRACT

Photoacoustic imaging of breast microcalcifications: A preliminary study with 8-gauge core-biopsied breast specimens

Ga Ram Kim

Department of Medicine
The Graduate School, Yonsei University

(Directed by Professor Eun-Kyung Kim)

Purpose: To present the photoacoustic imaging (PAI) tool and to evaluate whether microcalcifications in breast tissue can be detected on PA images.

Materials and methods: We collected 21 cores containing microcalcifications (n=11, microcalcification group) and none (n=10, control group) in stereotactic or ultrasound (US) guided 8-gauge vacuum-assisted biopsies. Photoacoustic (PA) images were acquired through ex vivo experiments by transmitting laser pulses with two different wavelengths (700nm and 800nm). The presence of microcalcifications in PA images were blindly assessed and compared with specimen mammography. A ratio of the signal amplitude occurring at 700nm to that occurring at 800nm was calculated for each PA focus and was called the PAI ratio.

Results: Each PA focus of the cores in the microcalcification group was matched against existing microcalcifications on specimen mammography. Based on the spectral change of PA signal amplitude between 700 nm and 800 nm, 10 out of 11 specimens containing microcalcifications and 8 out of 10 specimens without calcifications

were identified correctly by two blinded radiologists; the sensitivity, specificity, accuracy, positive predictive and negative predictive values of our blind review were 90.91%, 80.0%, 85.71%, 83.33% and 88.89%. The PAI ratio in the microcalcification group was significantly higher than that in the control group (the median PAI ratio, 2.46 versus 1.11, respectively, *P*= .001).

Conclusion: Breast microcalcifications generated distinguishable PA signals unlike breast tissue without calcifications. So, PAI, a non-ionizing and non-invasive hybrid imaging technique, can be an alternative in overcoming the limitations of conventional US imaging.

Key words : breast, microcalcifications, photoacoustic imaging, ultrasound, mammography

Photoacoustic imaging of breast microcalcifications: A preliminary study with 8-gauge core-biopsied breast specimens

Ga Ram Kim

Department of Medicine
The Graduate School, Yonsei University

(Directed by Professor Eun-Kyung Kim)

I. INTRODUCTION

Mammographic lesions manifested by microcalcifications constitute approximately half of clinically occult breast cancers and are frequently employed as an indicator of early breast cancer.[1-3] If microcalcifications detected on mammography are deemed suspicious for malignancy, a biopsy is required and recently, among a variety of biopsy approaches, vacuum-assisted biopsy with stereotactic guidance is mainly chosen. Even though this method is successful in aiding the diagnosis of breast microcalcifications, stereotactic guidance requires mammographic compression and radiation exposure of the breast. [4,5] In general, ultrasound (US)-guided vacuum-assisted biopsy is preferred over mammographic guidance because US guidance offers a number of advantages over stereotactic guidance: patients can be in a supine position without compression of the breast and radiation hazards; images of the procedures can be acquired in real time.[4-7] Although the low visibility of microcalcifications can be one of the biggest drawbacks of US imaging due to its relative low contrast resolution, US-guided vacuum-assisted biopsy can be an effective alternative to stereotactic-guided vacuum-assisted biopsy in the cases where microcalcifications are visible on US.[6,8-10]

Since photoacoustic imaging (PAI) is a real-time molecular imaging modality with high spatial and contrast resolutions, it may be an alternative for the imaging of breast microcalcifications in real time.[11-13] The PAI technology has been applied to various areas, such as tumor angiogenesis studies, functional brain studies, and deep internal organ imaging in animals.[13-15] Previous studies about PAI for real-time detection of breast microcalcifications were performed in order to determine optimal laser wavelength that was found to be 700 nm. In fact, the laser energy absorbance consistently decreases from 700 nm to the near-infrared spectrum range. By using the unique absorbance spectrum, 3-dimentional spectroscopic photoacoustic (PA) images of breast specimens were proposed.[16,17]

In this paper, we present the PAI tool and evaluate whether microcalcifications in breast tissue can be detected on PA images.

II. MATERIALS AND METHODS

1. Study Sample

The study was approved by the Institutional Review Board. All patients were informed about their inclusion in the study. Written consent was obtained from all subjects prior to their biopsy procedures.

Among patients who were scheduled to undergo sequential 8-gauge vacuum-assisted core needle biopsy procedures with stereotactic guidance or US guidance for breast microcalcifications suspected to be malignancy by mammography (Breast Imaging Reporting and Data System [BI-RADS] category 4 or 5), 11 patients agreed to participate in our study from April 2012 to March 2013 and they were prospectively included in the microcalcification group (all female; age, 31-74 years). Eleven cores from the 11 patients were obtained and specimen mammography was performed to confirm the presence of microcalcifications in core samples. The control group consisted of 5

patients (all female; age, 24-41 years) undergoing sequential 8-gauge vacuum-assisted core needle excision procedures with US guidance for biopsy-proven fibroadenoma during the same period. These patients were also prospectively included in our control group with their consent. Specimen mammography of the 10 cores obtained from the 5 patients was performed to confirm that the cores of the control group revealed no microcalcifications. In all, 21 cores of breast tissue were obtained from the 16 patients who were included in our study. Mammography was performed using the Selenia full field digital mammography system (Lorad/ Hologic, Danbury, Conn). To allow correlation between the two modalities, specimen mammographic images were acquired in 2 view image planes: top-down and lateral view. The number and size of calcifications on each specimen mammography were recorded. The size of each calcification in the cores of the microcalcification group was assessed using the longest diameter of each calcification focus shown on specimen mammography.

2. Imaging System and Experimental Procedures

The experimental arrangement of the photoacoustic (PA) and US imaging data acquisition system was assembled using a commercial US unit (Figure 1.). The specimens were set on a scatter-free gel pad (Parker Lab, Inc., Farfield, NJ, USA), which was immersed in a 0.9% saline-filled container. The temperature of the container was stably maintained at 24℃. To acquire PA signals from the specimens, radiofrequency (RF) data were captured with a commercial US scanner equipped with a SonixTouch research package (Ultrasonix Corp., Vancouver, BC, Canada) and a 7-MHz linear array (L14-5/38) connected to a SonixDAQ parallel system. The Q-switch trigger of a Nd:YAG laser excitation system (Surelite III-10 and Surelite OPO Plus, Continuum Inc., Santa Clara, CA, USA) was sent to a SonixTouch research

package. Whenever the US scanner received the scanline-generation trigger, scanline RF data were acquired. The pulse length of the emitted laser was 7 ns and its wavelength was controlled by a software program in a personal computer. The distance between the array transducer and breast specimen was fixed at 30 mm that was longer than the transducer's elevational focal depth of 16 mm. Note that laser delivery was conducted by a custom bifurcated optic fiber bundle and their optical fluency was focused at 30 mm depth from the array transducer (Fiberoptic Systems, Inc., Simi Valley, CA, USA). The imaging reconstruction was conducted with an optimal sound speed of 1500 m/s.[18] Before performing experiments to acquire PA signals, specimens were steeped in saline solution for about 6 hours in order to exclude potentially-remaining blood. This procedure was required when only investigating PA signals generated from microcalcifications without any interference from hemoglobin in blood.

(a)

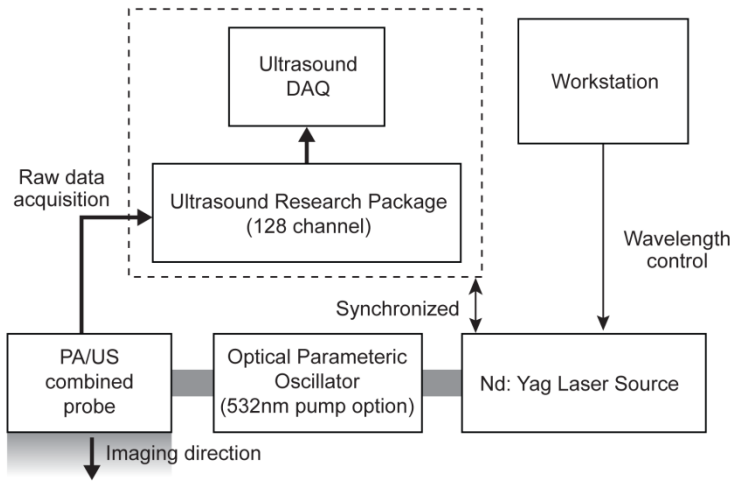

(b)

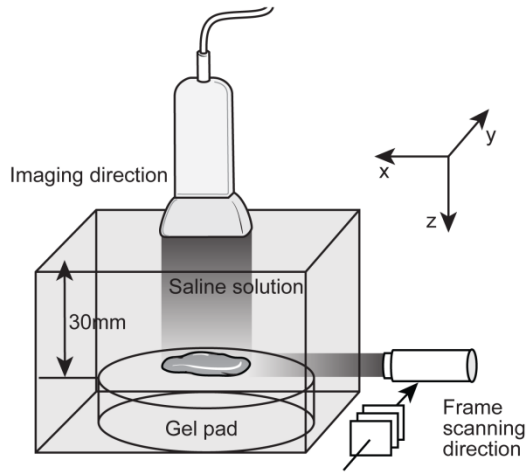

Figure 1. Diagram demonstrates experimental arrangement (a) to acquire photoacoustic signal images from 8-gauge core-biopsied breast specimens (b). To obtain 3-dimensional photoacoustic data, the probe was mechanically moved along the frame scanning direction (b).

The locations of the breast microcalcifications that appeared in PA images were verified by comparing them with those in mammography. For this, 3-dimensional PA images were acquired through mechanical scanning along the elevation direction of an US array transducer at 0.3 mm increments. For 3-dimensional data, the XYZ-axis mechanical scanner and its driver (SGSP26-100 and SHOT-204MS, Sigma Koki, Co., Ltd., Tokyo, Japan) were implemented with LabVIEW software (National Instruments, Corp., Austin, TX, USA). With the acquired 3-dimensional RF data from the experimental setup, projected PA images in top-down and lateral directions were reconstructed through a programmed software of MATLAB (Mathworks, Inc., Natick, MA, USA).

A previous study had demonstrated that microcalcifications in the breast tissue highly absorb laser pulses having a 700 nm wavelength and that the laser energy absorbance consistently decreased from 700 nm to the near infrared range.[16] Based on this result, PA signals were generated by transmitting laser pulses with two different wavelength sections as follows:

700 nm and 800 nm. Additional PA images were acquired by subtracting the two PA images derived from the two distinct wavelengths. The researchers performing all experimental procedures were blinded to the findings of specimen mammography.

3. Data Analyses

After the experiments were done, 2 radiologists blindly reviewed 3-dimensional PAI data of each core in order to identify microcalcifications within the core and to verify their locations. The presence and location of microcalcifications in PA images of each core were determined when the two radiologists reached an agreement. They found foci that showed PA signals with maximal amplitude on 700 nm and decreased or disappeared PA signals on 800 nm. Each core was then placed into one of two groups after completion of the blind review: those with assumed microcalcifications detected on PA images or those with no microcalcifications identified on PA images. The presence and location of microcalcifications appearing in PA images were demonstrated by comparing them with those in specimen mammography. To verify this visual assessment, we measured quantitative PA spectral responses from selected regions of interest (ROIs) which were drawn manually in the core and calculated the ratio of the amplitude occurring at the 700 nm wavelength section to the amplitude occurring at the 800 nm wavelength section of each focus. The ratio was called a PAI ratio in this paper.

Continuous data are presented as medians (with ranges). Comparisons between the control group and microcalcification group were performed using the Mann-Whitney U test for continuous variables. In the microcalcification group, multiple regression analysis estimated the relationship between the PAI ratio and other variables. Analysis was

performed using SPSS® statistical software (SPSS Inc., Chicago, IL, ver 20.0), and statistical significance was accepted as p-value < 0.05.

III. RESULTS

1. Baseline Characteristics

The average age of the 16 patients in this study was 43.81 years (24-74 years). The 11 patients included in the microcalcification group were diagnosed as follows: ductal carcinoma in situ (DCIS) (n=5), fibrocystic change (n=4), sclerosing adnenosis (n=1), and columnar cell change (n=1).

Each focus of the cores assumed to be found with microcalcifications detected on PA images was matched against existing microcalcifications confirmed by specimen mammography. Table 1 summarizes our 21 cases and shows whether microcalcifications were identified or not on PA images and specimen mammography. The number of calcifications-foci of each core in the microcalcification group ranged from 1 to 45 (mean number, 21.73). The median size of calcifications within the cores is also summarized in Table 1 and ranges from 130 to 500㎛.

Table 1. Baseline characteristics of 21 cases of the control and microcalcification groups

Case	age	Pathologic diagnosis	Assumed calcification on PAI[1]	Confirmed calcification on specimen mammography		
				Existence	Number	Size [2]
1	25	Fibroadenoma	No	No	-	-
2	43	Ductal carcinoma in situ	Yes	Yes	10	500 (210-830)
3	25	Fibroadenoma	No	No	-	-
4	24	Fibroadenoma	No	No	-	-

5	39	Fibroadenoma	No	No	-	-
6	31	Fibrocystic change	Yes	Yes	45	310 (190-940)
7	41	Fibroadenoma	No	No	-	-
8	43	Fibrocystic change	Yes	Yes	17	130 (90-220)
9	49	Ductal carcinoma in situ	Yes	Yes	16	160 (70-260)
10	41	Fibroadenoma	Yes	No	-	-
11	42	Fibrocystic change	Yes	Yes	41	325 (160-390)
12	47	Ductal carcinoma in situ	Yes	Yes	27	220 (110-250)
13	24	Fibroadenoma	No	No	-	-
14	48	Ductal carcinoma in situ	Yes	Yes	14	280 (140-430)
15	24	Fibroadenoma	Yes	No	-	-
16	29	Fibroadenoma	No	No	-	-
17	41	Fibroadenoma	No	No	-	-
18	46	Columnar cell change	Yes	Yes	1	230
19	59	Sclerosing adenosis	Yes	Yes	22	220 (80-760)
20	39	Fibrocystic change	No	Yes	29	265 (120-390)
21	74	Ductal carcinoma in situ	Yes	Yes	17	290 (110-1000)

[1] Photoacoustic Imaging.

[2] Median value (range) of the diameter in calcifications (㎛).

2. Detection of Microcalcifications on Photoacoustic Images

Based on the spectral change of PA signal amplitude between 700 nm and 800 nm, 10 out of 11 specimens containing microcalcifications were chosen correctly by the two radiologists identifying the right location of the microcalcifications and 8 out of 10 specimens without calcifications were also identified correctly by the radiologists (Table 2); the sensitivity, specificity, accuracy, positive predictive and negative predictive values of our blinded review were 90.91%, 80.0%, 85.71%, 83.33% and 88.89%, respectively. With regard to the quantitative analysis of PA spectral change, the cores in the microcalcification group showed decreasing PA intensities in the ROI which was proven to be the region containing microcalcifications by specimen mammography (compare Fig 2b. and Fig 2c.). On the other hand, the cores belonging to the control group showed constant PA intensities from

unidentified foci (compare Fig 3b. and Fig 3c.). Their spectral changes are summarized in Figure 4. In addition to raw PA images, we subtracted the PA signal amplitude at 800 nm from that at 700 nm, which was called spectroscopic imaging; this subtraction of PA images were combined with conventional gray scale US images to aid in the determination of microcalcifications (Fig 2d. and Fig 3d.).

Table 2. Results of blind review to assume calcification on PAI[1]

Presence of Calcification		Calcification on Specimen mammography		Total
		Yes	No	
Calcification on PAI[1]	Yes	10	2	12
	No	1	8	9
Total		11	10	21

[1] Photoacoustic Imaging.

(a)

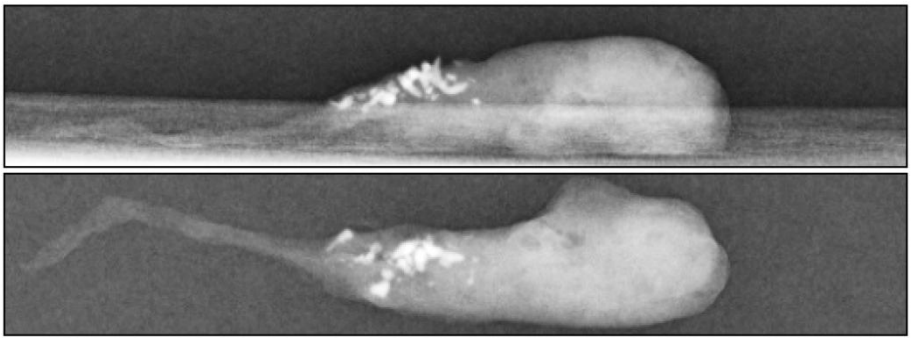

(b)

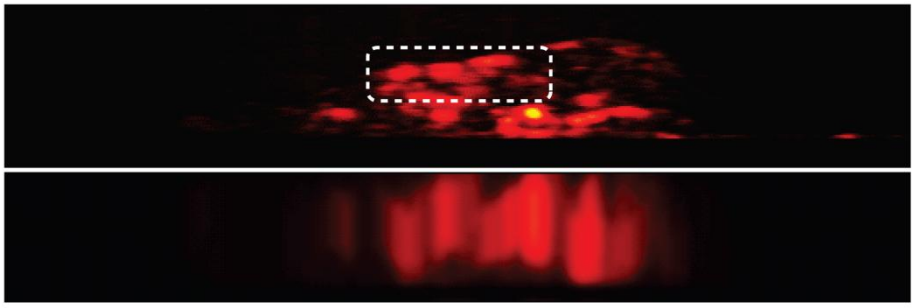

(c)

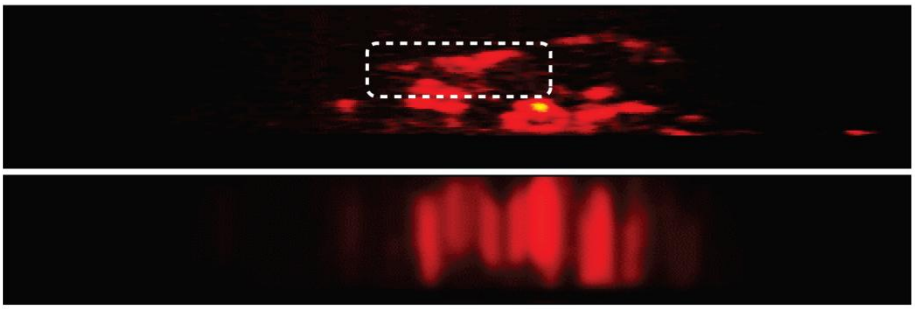

(d)

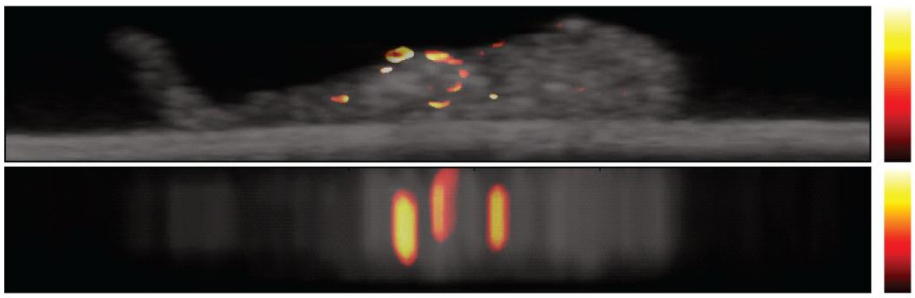

Figure 2. Representative case from ex vivo experiments with core specimens of breast tissue included in the microcalcification group (case #2). Specimen mammography (a) and photoacoustic images obtained from both 700 nm (b) and 800 nm (c) wavelengths were reconstructed with comparable configurations in both directions (top-down and lateral views). The locations of photoacoustic signals were well matched with microcalcifications observed in specimen mammography. The photoacoustic image at 800 nm (c) showed decreasing photoacoustic signal intensities in the region confirmed as microcalcifications through specimen mammography compared with the photoacoustic image at 700 nm (b). The mean value of PAI ratio[†] from region of interest was 2.80. The subtraction PA image of 700 nm and 800 nm was

reconstructed and combined with a conventional gray scale US image (d). *PAI ratio* = Calculated ratio of the amplitude occurring at the 700 nm wavelength section to that occurring at the 800 nm wavelength section

(a)

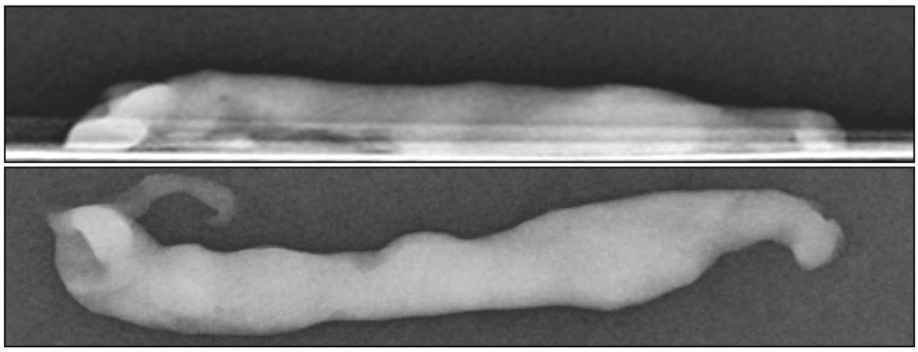

(b)

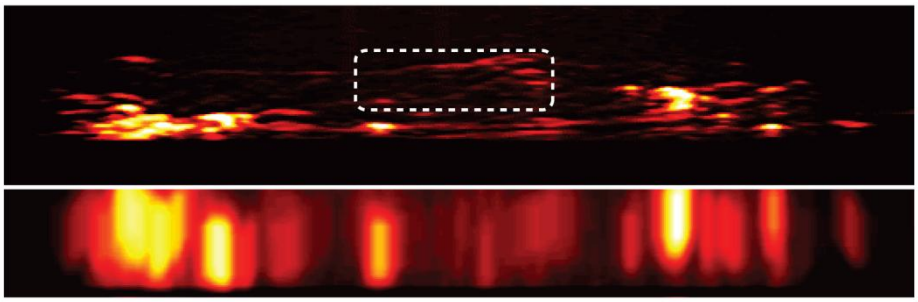

(c)

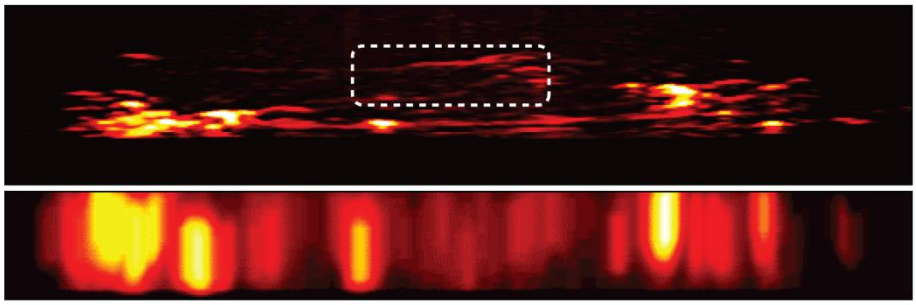

(d)

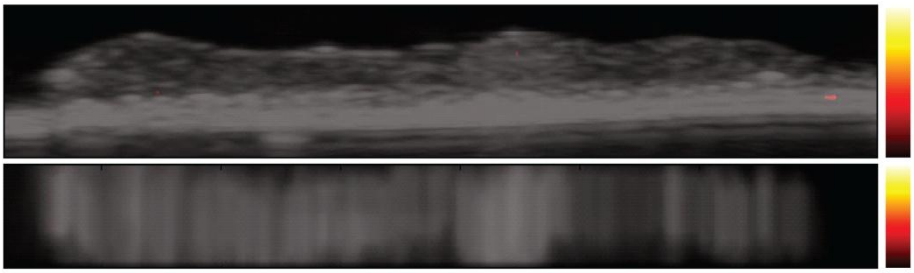

Figure 3. Representative case from ex vivo experiments with core specimens of breast tissue included in the control group (case #5). Specimen mammography (a) and photoacoustic images (b,c) were reconstructed with comparable configurations in both directions (top-down and lateral views). The photoacoustic image at 800 nm (c) shows constant photoacoustic signal intensities from an unidentified target compared with the photoacoustic image at 700 nm (b). The signal foci in the region of interest are assumed to be in the core. All these foci show constant photoacoustic intensities. The mean value of PAI ratio[†] from region of interest within this core was 1.21. The other bright signal foci around the core may be photoacoustic signals from the interfaces between the surfaces of specimen and the gel pad, which show grossly constant photoacoustic signal intensities. The subtraction photoacoustic image was reconstructed and combined with a conventional gray scale US image (d). *PAI ratio* = Calculated ratio of the amplitude occurring at the 700 nm wavelength section to that occurring at the 800 nm wavelength section

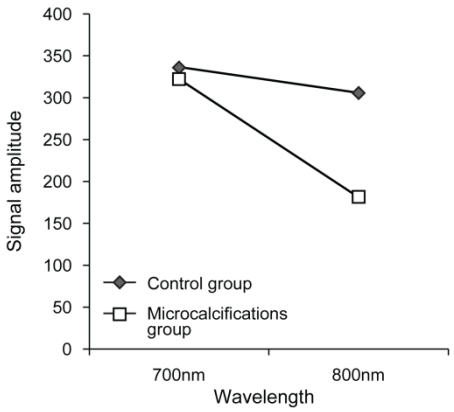

Figure 4. Spectral change in mean values of the maximum photoacoustic signals at the 700 nm and 800 nm wavelength sections in the control and microcalcification group.

3. Comparison of Quantitative Photoacoustic Spectral Responses

To verify these spectral changes in PA amplitude, we calculated the PAI ratios of specimens included in the microcalcification group and those of specimens included in the control group. All mean values of PAI ratios from regions of interest within each core are summarized in Table 3. The PAI ratio in the microcalcification group was significantly higher than the PAI ratio of cores included in the control group (median PAI ratio [range], 2.46 [1.03-3.92] versus 1.10 [0.93-1.21], *P*=0.006), respectively (Figure 5.).

Table 3. PAI ratios[1] from regions of interest within each core

Control group		Microcalcification group		*P* value
Case number	PAI ratio[1]	Case number	PAI ratio[1]	
1	1.18	2	2.80	
3	1.14	6	2.63	
4	1.06	8	3.19	
5	1.21	9	1.68	
7	1.08	11	3.0	
10	1.12	12	1.79	
13	1.11	14	2.46	
15	0.93	18	1.03	
16	1.10	19	3.92	
17	1.03	20	1.06	
		21	1.60	
Median value (range)	1.10 (0.93-1.21)	Median value (range)	2.46 (1.03-3.92)	0.006

[1] Mean values of PAI ratios (The ratio of the amplitude occurring at the 700 nm wavelength section to that occurring at the 800 nm wavelength section) calculated from each core.

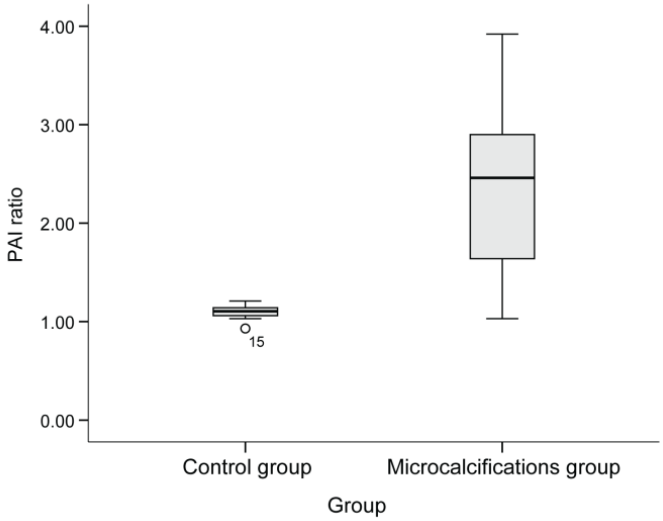

Figure 5. The PAI ratio in the microcalcification group was significantly higher than that in the control group. *PAI ratio* = Calculated ratio of the amplitude occurring at the 700 nm wavelength section to that occurring at the 800 nm wavelength section

To discover factors that contribute to PAI ratios, we performed an additional subgroup analysis in the microcalcification group. We used a multivariable regression model with the dependent variable of the PAI ratio and the independent predictors of other variables (malignancy, number and size of calcifications-foci). On multiple regression analysis, neither malignant diagnosis nor the number or size of calcification-foci was proven to contribute to PAI ratios (Table 4).

Table 4. Multiple regression analysis in the microcalcification group (n=11) to find factors that contribute to PAI ratios[1]

	Beta (standard error)	P value
Variables		
Malignant diagnosis[2]	-0.346 (0.707)	0.639
Number of calcification-foci in	0.001 (0.004)	0.717

the core‡		
Size of calcification-foci in the core[3]	0.013 (0.028)	0.653

[1] Calculated ratio of the amplitude occurring at the 700 nm wavelength section to that occurring at the 800 nm wavelength section.
[2] Malignant result according to the pathology report.
[3] Median value of calcification-foci in the core.

IV. DISCUSSION

Visualization of microcalcifications by US examination has been improved due to the development of high resolution US.[4,7,19-21] However, the current US technology is still considered to be an unreliable method for the detection or evaluation of microcalcifications compared to mammography in clinical use.[7,10,20-25] A new commercial image processing technique to show more microcalcifications than gray scale US was proposed before, but it was merely an integrated software program that used a filter technique in order to detect only isolated points using higher brightness compared to the surrounding breast tissue.[26] Performers could become confused because of clustered microcalcifications or hyperechoic background including glandular and fibrous tissue.[26] Thus, an imaging technique intrinsically based on microcalcifications is indeed required.

PAI is an emerging technology combining the merits of both light and US, and its images are based on the microcalcifications themselves. The idea of microcalcifications being imaged by PA technology was first derived from absorbance differences between microcalcifications and hemoglobin. PA technology has imaged the hemoglobin distribution and oxygenation state inside breast tissue, and the main absorbers within normal breast tissue were deoxy- and oxy-hemoglobin.[27-29] Different molecules have distinguishing absorption spectra in response to different laser emissions. As a result, the characteristic absorption spectrum of microcalcifications in response to a

specific wavelength of laser pulse allows PA signals to be distinguishable compared to surrounding tissues. PA intensity from microcalcifications was found to be differentiated from that of background tissue with the wavelength 700 nm and 800 nm.[16] Similarly, the difference of PA intensity between 700 nm and 800 nm in the microcalcification group was larger than that in the control group with statistical significance in this study.

This study assessed the feasibility of PAI to detect breast microcalcifications which were well correlated with detection results of specimen mammography. Curiously enough, the cores of both the microcalcifications and control group presented unidentified PA signal foci because all molecules, including not only microcalcifications but also surrounding tissues in the core, generated PA signals in response to the emitted laser. In addition, unspecified PA signal foci may also originate from the interfaces between the surfaces of the specimen and the saline containing the specimen or the gel pad supporting the specimen. But, these unspecified foci disclosed constant PA signal intensities regardless of wavelength change whereas PA intensities obtained from ROIs of microcalcifications showed characteristic spectral change (median PAI ratio, 1.11 in the control group versus 2.46 in the microcalcification group, P=.001). As a result, a practical measure to ensure that clear PA images are obtained from just microcalcifications is urgently needed when PAI is applied to human breasts in vivo. Subtraction images can be reconstructed with the spectral difference of PA intensities in microcalcifications and this will allow enhancing contrast resolution.

In this study, with the use of PAI, a sensitivity of 90.91% and a specificity of 80.0% for detection of microcalcifications within the specimens were achieved although false positive (n=2) and false negative (n=1) results were found. This may be because the blinded review to find microcalcifications on PA images did depend on the gross judgment of the

two radiologists. The subtraction images derived from the calculated PAI ratio would make it easier for performers to detect microcalcifications during the conventional US examination. However, technical improvements to emphasize and maximize contrast between microcalcifications and surrounding tissues are necessary since the broad range of PAI ratio in the microcalcification group was shown to be from 1.03 to 3.92, in which there are overlaps with the control group.

There have been several attempts to identify underlying biochemical differences that distinguish benign from malignant microcalcifications, but a definite difference in chemical composition has not been clarified yet.[30-34] Two major types of microcalcifications found in breast tissue (calcium oxalate and hydroxyapatite) have been investigated by Raman spectroscopy.[11,35-37]. Unfortunately, we were unable to analyze the chemical composition of calcifications inside the cores on histopathology. Instead, we intended to find factors contributing to different PA signal amplitudes of calcifications, especially including malignant diagnosis as one of the independent predictors. However, we failed to discover any significant factors among variables such as malignant diagnosis as well as the number and size of calcification-foci in the subgroup analysis (n=11). According to previous reports,[17] PAI ratios of malignant and benign microcalcifications have the potential to be different if malignant and benign calcifications are truly distinct. In order to clarify the difference of PAI ratio according to the intrinsic character of calcifications, we will need to perform PAI with increased sample size and should measure the quantitative spectral response of calcium oxalate and hydroxyapatite in the future; their absorbance features might differentiate each other, which is consistent with previous reports about calcium oxalate and hydroxyapitite in breast lesions. [3,30,35,38]

Our study still has a number of limitations. First of all, our sample size is relatively small as it is one of the preliminary studies about PAI of

breast microcalcifications. Therefore, further studies with larger sample sizes will be necessary. Second, since this is a pilot study with biopsy specimens, practical application might still be limited. Further prospective studies should be performed by developing a sophisticated PA transducer and controlling unexpected properties of PA signals that might occur in its in-vivo use.

V. CONCLUSION

In conclusion, breast microcalcifications generated distinguishable photoacoustic signals unlike breast tissues without calcifications. So, PAI, a non-ionizing and non-invasive hybrid imaging technique, can propose an alternative in overcoming the limitations of the conventional US imaging.

REFERENCES

1. Meyer JE, Eberlein TJ, Stomper PC, Sonnenfeld MR. Biopsy of occult breast lesions. Analysis of 1261 abnormalities. JAMA (Chicago, Ill.) 1990;263:2341-3.
2. Liberman L, Abramson AF, Squires FB, Glassman JR, Morris EA, Dershaw DD. The breast imaging reporting and data system: positive predictive value of mammographic features and final assessment categories. AJR Am J Roentgenol 1998;171:35-40.
3. Baker R, Rogers KD, Shepherd N, Stone N. New relationships between breast microcalcifications and cancer. British Journal of Cancer 2010;103:1034-9.
4. Soo MS, Baker JA, Rosen EL. Sonographic detection and sonographically guided biopsy of breast microcalcifications. AJR Am J Roentgenol 2003;180:941-8.
5. Parker SH, Burbank F. A practical approach to minimally invasive breast biopsy. Radiology 1996;200:11-20.
6. Kim HS, Kim MJ, Kim EK, Kwak JY, Son EJ, Oh KK. US-guided vacuum-assisted biopsy of microcalcifications in breast lesions and long-term follow-up results. Korean Journal of Radiology 2008;9:503-9.
7. Soo MS, Baker JA, Rosen EL, Vo TT. Sonographically guided biopsy of suspicious microcalcifications of the breast: a pilot study. AJR Am J Roentgenol 2002;178:1007-15.
8. Liberman L. Percutaneous image-guided core breast biopsy. Radiologic clinics of North America 2002;40:483-500, vi.
9. DeAngelis GA, Moran RE, Fajardo LL, Mugler JP, Christopher JM, Harvey JA. MRI-guided needle localization: technique. Seminars in ultrasound, CT, and MRi 2000;21:337-50.
10. Youk JH, Kim EK, Kim MJ, Lee JY, Oh KK. Missed breast cancers at US-guided core needle biopsy: how to reduce them. Radiographics 2007;27:79-94.
11. Baker M. Whole-animal imaging: The whole picture. Nature 2010;463:977-80.
12. Zhang HF, Maslov K, Stoica G, Wang LV. Functional photoacoustic microscopy for high-resolution and noninvasive in vivo imaging. Nat Biotechnol 2006;24:848-51.
13. Kong F, Chen YC, Lloyd HO, Silverman RH, Kim HH, Cannata JM, et al. High-resolution photoacoustic imaging with focused laser and ultrasonic beams. Appl Phys Lett 2009;94:33902.
14. Ku G, Wang X, Xie X, Stoica G, Wang LV. Imaging of tumor angiogenesis in rat brains in vivo by photoacoustic tomography. Applied optics 2005;44:770-5.

15. Song KH, Wang LV. Noninvasive photoacoustic imaging of the thoracic cavity and the kidney in small and large animals. Medical physics 2008;35:4524-9.
16. Kang J, Kim E-K, Young Kwak J, Yoo Y, Song T-k, Ho Chang J. Optimal laser wavelength for photoacoustic imaging of breast microcalcifications. Applied Physics Letters 2011;99:153702--3.
17. Kang J, Kim E-k, Kim GR, Yoon C, Song T-k, Chang JH. Photoacoustic imaging of breast microcalcifications: A validation study with 3-dimensional ex vivo data and spectrophotometric measurement. Journal of Biophotonics 2013. DOI 10.1002/jbio.201300100
18. Yoon C, Kang J, Han S, Yoo Y, Song T, Chang JH. Enhancement of photoacoustic image quality by sound speed correction: ex vivo evaluation. Optics express 2012;20:3082-90.
19. Moon WK, Im JG, Koh YH, Noh DY, Park IA. US of mammographically detected clustered microcalcifications. Radiology 2000;217:849-54.
20. Anderson ME, Soo MS, Bentley RC, Trahey GE. The detection of breast microcalcifications with medical ultrasound. J Acoust Soc Am 1997;101:29-39.
21. Yang WT, Suen M, Ahuja A, Metreweli C. In vivo demonstration of microcalcification in breast cancer using high resolution ultrasound. Br J Radiol 1997;70:685-90.
22. Huang CS, Wu CY, Chu JS, Lin JH, Hsu SM, Chang KJ. Microcalcifications of non-palpable breast lesions detected by ultrasonography: correlation with mammography and histopathology. Ultrasound Obstet Gynecol 1999;13:431-6.
23. Park JS, Park YM, Kim EK, Kim SJ, Han SS, Lee SJ, et al. Sonographic findings of high-grade and non-high-grade ductal carcinoma in situ of the breast. J Ultrasound Med 2010;29:1687-97.
24. Ranieri E, D'Andrea MR, D'Alessio A, Bergomi S, Caprio G, Calabrese GB, et al. Ultrasound in the detection of breast cancer associated with isolated clustered microcalcifications, mammographically identified. Anticancer Res 1997;17:2831-5.
25. Hendrick RE. Radiation doses and cancer risks from breast imaging studies. Radiology 2010;257:246-53.
26. Machado P, Eisenbrey JR, Cavanaugh B, Forsberg F. New image processing technique for evaluating breast microcalcifications: a comparative study. J Ultrasound Med 2012;31:885-93.
27. Manohar S, Vaartjes SE, van Hespen JC, Klaase JM, van den Engh FM, Steenbergen W, et al. Initial results of in vivo non-invasive cancer imaging in the human breast using near-infrared photoacoustics. Opt Express 2007;15:12277-85.
28. Kruger RA, Lam RB, Reinecke DR, Del Rio SP, Doyle RP.

Photoacoustic angiography of the breast. Med Phys 2010;37:6096-100.
29. Ermilov SA, Khamapirad T, Conjusteau A, Leonard MH, Lacewell R, Mehta K, et al. Laser optoacoustic imaging system for detection of breast cancer. J Biomed Opt 2009;14:024007.
30. Morgan MP, Cooke MM, McCarthy GM. Microcalcifications associated with breast cancer: an epiphenomenon or biologically significant feature of selected tumors? J Mammary Gland Biol Neoplasia 2005;10:181-7.
31. Menges V, Busing CM, Hirsch O. [The diagnostic value of mammographic signs of malignancy in clinically occult breast carcinoma (author's transl)]. Rofo 1981;135:482-9.
32. Tornos C, Silva E, el-Naggar A, Pritzker KP. Calcium oxalate crystals in breast biopsies. The missing microcalcifications. Am J Surg Pathol 1990;14:961-8.
33. Going JJ, Anderson TJ, Crocker PR, Levison DA. Weddellite calcification in the breast: eighteen cases with implications for breast cancer screening. Histopathology 1990;16:119-24.
34. Frouge C, Meunier M, Guinebretiere JM, Gilles R, Vanel D, Contesso G, et al. Polyhedral microcalcifications at mammography: histologic correlation with calcium oxalate. Radiology 1993;186:681-4.
35. Haka AS, Shafer-Peltier KE, Fitzmaurice M, Crowe J, Dasari RR, Feld MS. Identifying microcalcifications in benign and malignant breast lesions by probing differences in their chemical composition using Raman spectroscopy. Cancer Res 2002;62:5375-80.
36. Saha A, Barman I, Dingari NC, McGee S, Volynskaya Z, Galindo LH, et al. Raman spectroscopy: a real-time tool for identifying microcalcifications during stereotactic breast core needle biopsies. Biomedical Optics Express 2011;2:2792-803.
37. Krishna CM, Kurien J, Mathew S, Rao L, Maheedhar K, Kumar KK, et al. Raman spectroscopy of breast tissues. Expert Rev Mol Diagn 2008;8:149-66.
38. Stone N, Baker R, Rogers K, Parker AW, Matousek P. Subsurface probing of calcifications with spatially offset Raman spectroscopy (SORS): future possibilities for the diagnosis of breast cancer. Analyst 2007;132:899-905.

ABSTRACT(IN KOREAN)

유방 미세석회화의 광음향초음파 영상: 8 게이지 핵심생검 유방검체를 이용한 예비연구

<지도교수 김은경>

연세대학교 대학원 의학과

김가람

목적: 유방촬영술에서 보이는 유방의 미세석회화 병변에 대하여 광음향초음파를 이용한 초음파 영상을 구현하여 유방조직의 석회화를 영상으로 구현한다.
방법: 연구기간 동안 유방촬영술상 유방암의증 국소 미세석회화 병변이 있어서 8 게이지 맘모톰 조직검사의 시행한 환자 11 명에서 11 개의 검체를 석회화군으로 포함시킨다. 같은 기간동안 조직검사로 섬유선종으로 진단되어 맘모톰 절제를 시행하는 환자 5 명에서 얻은 10 개의 검체를 대조군으로 포함시킨다. 이들 총 21 개의 검체가 본 연구의 대상이 되었으며 검체유방촬영술을 시행한 후 생체외 실험을 통해 광음향초음파 영상을 얻는다. 21 개 검체의 광음향초음파 영상에 대한 블라인드 테스트를 시행하여 석회화의 유무를 가려낸다. 700nm 와 800nm 파장대에서 광음향신호의 최고진폭을 각각 측정하여 그 비를 계산하고 이를 광음향비라고 칭한다.
결과: 석회화군에 포함된 검체 내의 광음향신호는 검체유방촬영술에 관찰되는 석회화와 잘 매치되었다. 블라인드 테스트 결과, 민감도, 특이도, 정확도, 양성예측도, 그리고 음성예측도는 90.91%, 80.0%, 85.71%, 83.33% 그리고 88.89%였다. 광음향비는 석회화군에서 2.3 으로 대조군(1.09)보다 유의확률 0.001 을 보이며 통계적으로 유의하게 높았다.

결론: 유방의 미세석회화는 석회화가 없는 유방조직과는 구별되는 광음향신호를 보였다. 이를 이용하여 유방 미세석회화에 대하여 기존 고식적 초음파의 한계를 극복하는 대안영상기법을 제안할 수 있다.

핵심되는 말 : 유방, 미세석회화, 광음향영상, 초음파, 유방촬영술